Numerical simulation of ammonia dispersion around a water curtain

O. Isnard, Lionel Soulhac, Gilles Dusserre

Numerical simulation of ammonia dispersion around a water curtain

O. Isnard [a,*], L. Soulhac [a], G. Dusserre [b]

[a] *Laboratoire de Mécanique des Fluides et d'Acoustique, École Centrale de Lyon, Université Claude Bernard, Lyon I, 36 av Guy de Collongue BP 163, 69131 Ecully, France*

[b] *Laboratoire Génie de l'Environnement Industriel, École Nationale Supérieure des Techniques et des Mines d'Alès, 6 av de Clavières 30100 Alès, France*

Abstract

Water curtains have been suggested as a way of limiting the spread of ammonia in the event of an accidental release. Several field experiments have already been performed to investigate the interaction between a water curtain and a cloud of ammonia, most recently by Bara and Dusserre (1997, *J. Loss Prev. Ind.*, 10(3), 179–183). Those experiments have been modelled numerically, using the computational code Mercure. The calculated velocities and concentrations agree reasonably well with the measurements.

Keywords: Water curtain; Ammonia; Dispersion

1. Introduction

Ammonia is used in a wide range of industrial processes, and it is commonly stored, in liquid form, under pressure, on industrial sites. It is also frequently transported by road and rail in pressurised containers. There are therefore many opportunities for accidental releases of ammonia, and such release can have very serious consequences. Ammonia is a highly toxic gas, and for an accidental release in the atmosphere, the safe concentration limit is likely to occur too far away from the source to permit direct intervention at the source. It has been suggested that vertical water curtains might be used to create 'protected regions' within the ammonia cloud to permit emergency services to approach the source much more closely, and to protect vital installations.

The atmospheric dispersion of ammonia has been studied extensively using both experimental and numerical approaches. Recently Nielsen et al. (1997) published a review of field experiments set up during the CEC Environment project 'Fladis Field Experiments'. The main objective of these experiments was to study all stages in the dispersion of ammonia, over a flat terrain, from its release as liquified ammonia to a state of essentially passive dispersion. This study is particularly concerned with the use of a water curtain to modify the dispersion of ammonia. There have been several wind tunnel studies of the interaction between a dense gas cloud and an obstacle such as a fence (see Davies (1992) for an analysis of some of these experiments) and Papaspyros, Papanicolaou, Kastrinakis and Nychas (1996) report some wind tunnel studies of the effect of obstacles on the dispersion of ammonia. In particular, they concluded that the obstacle enhances the mixing and the dispersion of gas cloud. There have also been some field studies of the use of water curtains to limit the dispersion of various gases (e.g. Blewitt, Yohn, Koopman, Brown & Hague, 1987), but as far as we are aware, the only field study of the use of water curtains with ammonia releases is that reported by Bara and Dusserre (1997). The aim of their experiments was to study the effect of a water curtain on the dispersion of a cloud of ammonia gas, released upstream of the water curtain. The water curtain modifies the dispersion in two major ways. Firstly, the airflow transporting the ammonia must pass around or over the water curtain. This creates a

* Corresponding author. Tel.: + 33 4 72 18 63 03; fax: + 33 4 78 33 1380.

region in the wake of the water curtain which is largely protected from direct exposure to the gas cloud. Most of the transport into this region is by turbulent diffusion, although, as we shall see later, it is possible for the mean streamlines to penetrate the region. The pollutant which does enter the wake region is then mixed rather uniformly throughout the region, by the recirculating flow and the relatively high levels of turbulence, before leaving into the external flow. The droplets in the water curtain may contribute to a reduction in the ammonia concentration by absorbing ammonia vapour.

In order to assess the performance of the water curtain, we need to know the extent of the region protected by the water curtain, the likely ammonia concentration within the protected region, and the typical 'retention time' of the pollutant in the protected region. Such quantities are extremely difficult to measure in full-scale experiments, so a numerical model can provide a great deal of useful information. We have therefore used an existing computational code—Mercure—which was developed for the simulation of flow in the atmospheric boundary layer (Buty, Caneil & Carissimo, 1988) to simulate four of the field experiments reported by Bara and Dusserre (1997). As a first approach we have modelled the water curtain as a solid, rigid obstacle having approximatively the same dimensions as those reported for the water curtain. We have therefore ignored the possible absorption of ammonia by the water droplets in the spray, the semi-porous nature of the water curtain, and any dynamic interaction between the water curtain and the incident wind. So an important, additional question concerns whether such a simplified model can represent a non-rigid, semi-porous structure such as a water curtain. In Section 2, we review the field experiments briefly, and then, in Section 3 we describe the numerical simulations. The computational results for the wind velocities are presented and discussed in Section 4, followed by the concentrations in Section 5.

2. The field experiments

The field experiments were carried out at a test site at Champelauson (Gard, France), and they have been described in detail by Bara and Dusserre (1997), so they will only be summarised here. The test site is a large rectangular area, with a surface consisting principally of dirt and gravel, giving an average roughness height of about 1 cm.

The ammonia was stored as a liquid in a pressurised bottle, and was discharged through the outlet valve at the top of the bottle as a jet. The bottle was inclined so that the jet impacted on the ground; some of the ammonia formed a pool on the ground, and the rest dispersed immediately, either as vapour or as aerosol. The release rate was very low—about 20 kg of liquified ammonia in 2 min—so it can be assumed that the aerosol cloud did not have any significant initial momentum.

The water curtain was located 8 m downwind of the source, and consisted of a horizontal water jet (at pressure of about 10 bar) which impacted on a vertical, semi-elliptical plate which deflected and dispersed the jet. The resultant spray formed a water curtain in the shape of a peacock's tail.

3. The numerical simulations

The calculations have been performed using the atmospheric boundary layer code Mercure (Buty *et al.*, 1988), which is a 3-dimensional model, based on a classical Navier–Stokes solver, with a standard k–ϵ turbulence model. The program uses a structured grid; for these calculations we used a mesh with 65 points in the streamwise direction, 27 points in the vertical and 61 points in the transverse direction (see Fig. 1). This corresponds to a physical domain measuring 100 m long, 80 m wide and 40 m high. The ground is assumed to be flat, with an aerodynamic roughness height of 1 cm; the air temperature was fixed at 20°C. The inflow condition consists of a logarithmic velocity profile, with a turbulence intensity of 25%. The pressure at the outflow from the domain is imposed, and is set equal to the atmospheric pressure (pressure of the ambient air at 20°C which follows the ideal gas law).

An important, and rather general, problem in modelling this type of flow is the representation of the water curtain. In reality, this consists of a rather thin sheet containing water droplets moving at high speed, which therefore acts as a porous screen. It has two important functions; the upward momentum of droplets (and the air that they entrain) acts as a vertical barrier to the flow, deflecting most it around the edges of the water curtain. The water droplets also play an important role in removing ammonia from the atmosphere, through the coalesc-

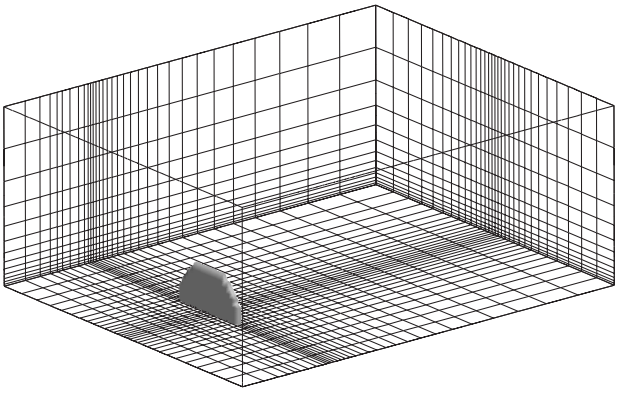

Fig. 1. Schematic view of the water curtain and the computational mesh. For clarity only every other grid point is shown.

ence of droplets and the absorption of ammonia vapour. These processes are essentially small-scale and rather complicated, and it is not possible to model them directly in calculations of atmospheric boundary layer flows in realistic, complex geometries. So one of the objectives of this work is to begin to consider how to model the effects of the water curtain in this type of calculation. We have therefore begun with the simplest possible approach; the water curtain is modelled as an impermeable barrier, with a slip condition for the velocity on the faces. The experiments (Bara & Dusserre, 1997) showed that the water curtain resembled a peacock's tail; we have therefore represented it as a semi-cylinder, with a radius of 10 m and a thickness of 60 cm.

4. The velocity field

The flow around a bluff body in the surface boundary layer is very complicated, and the detailed structure of the flow can depend rather sensitively on parameters such as the shape, size, porosity and orientation of the object. Hosker (1982) and Hunt (1984) provide comprehensive reviews of flow and dispersion round isolated obstacles. However, theoretical studies of dispersion in turbulent flows around bluff bodies (e.g. Puttock & Hunt, 1979; Puttock, 1979; Hunt & Mulhearn, 1973) suggest that the cross-sectional area of the pollutant cloud, and the concentrations, are determined mainly by the convergence and divergence of the mean streamlines, and do not depend too sensitively on the structure of the turbulence. Consequently, the quantities that are likely to be most important for a satisfactory prediction of pollutant concentrations will be the characteristic dimensions of the separation regions upstream and downstream of the water curtain.

Unfortunately, the velocity field around the water curtain was not measured during the field experiments—the only velocity that was measured was that of the incident wind upstream of the water curtain, at a height of 4 m. And since there do not seem to be any other published data sets of the velocity field around a water curtain, we have had to compare the results of our calculations with data for the flow around solid obstacles. This means that we have been unable to test our hypothesis that the water curtain can be modelled as a solid obstacle with a shear-free surface.

Most of the available data for the flow around bluff bodies are for objects for which the length (L) in the streamwise direction, is of the same order as the height (H) and width, (W). That is, the data have been obtained principally for objects with $L/H \geq 1$. We have modelled the water curtain as a rather thick 'plate', for which $L/H \sim 0.006$. The ratio L/H is important in that it determines whether the flow which separates upstream of the obstacle reattaches on the top or the sides of the obstacle, or whether the obstacle is enclosed in a single recirculation 'bubble'. Most measurements (e.g. Hosker, 1982) suggest that there will be no reattachment on the surface of the obstacle if $L/H < 1$ and $L/W < 1$. So we have compared our numerical results with data obtained for obstacles with $L/H \leq 1$ and $L/W \leq 1$.

4.1. Upwind separation

As the main flow approaches the water curtain it decelerates in the streamwise direction and accelerates vertically and laterally, so as to pass round the curtain. A standing eddy forms in front of the water curtain. This is illustrated in Fig. 2 which shows some of the mean streamlines in a view looking downwind towards the water curtain. The spiralling pattern of the streamlines immediately upwind of the water curtain illustrates the rather complex structure of the upwind vortex, and suggests that the vortex plays an important role in dividing the oncoming flow into the fraction that passes round the obstacle, and the fraction that passes over.

Previous wind tunnel studies have shown that the size and strength of the upwind vortex depends on the incident velocity profile relative to the body height. Corke and Nagib (1976) conducted wind tunnel studies on block-like obstacles in boundary layers with a range of different power-law velocity profiles ($u \propto z^n$). For the case closest to the one studied here ($n = 0.15$) they found that the upwind vortex extended to a height of about 0.6 H. Our numerical computations give a height of about 0.65 R (where R is the radius of the water curtain) which agrees reasonably well with the experimental data, since we can assume that our results should scale on R in much the same way as those for a rectangular object scale on H.

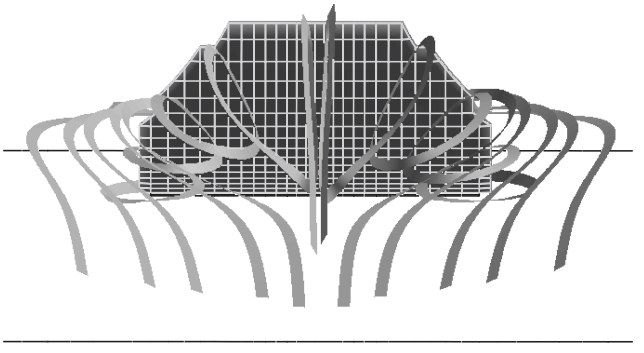

Fig. 2. Visualisation of the mean streamlines. View downwind, towards the water curtain.

4.2. Obstacle wake

The flow passing over and around the obstacle separates, creating a region of recirculating flow in the wake of the obstacle. If the obstacle is sufficiently short compared with its height and width ($L/H \leq 1$ and $W/H \leq 1$) then the length of the recirculation region (L_r) measured from the upwind face of the obstacle, should be relatively independent of L. Huber and Snyder (1976) measured L_r for a block-like structure ($L/H = 1$ and $W/H = 2$) and obtained $L_r/H \sim 2.5$. They also found that the maximum height (H_r) and half width (W_r) of the recirculating region were about 1.5 H, and occurred at a distance of about 1.5 H downwind of the upwind face of the obstacle. In these simulations, we obtain $L_r/R \sim 2.8$, and $W_r/R \sim 1.3$, which agree reasonably well with measured values.

The mean streamlines immediately downwind of the obstacle are rather complicated; Fig. 3 shows a view from downwind of the water curtain, looking upwind. Immediately behind the obstacle there is a large semi-toroidal vortex, which is visualised here as a surface of constant low pressure. This is consistent with other results which show the formation of a parallel pair of vertical vortex tubes immediately behind sharp edged bluff bodies (Woo, Peterka & Cermak, 1977). Since such structures cannot terminate in the fluid, they are therefore probably connected. The vertical nature of this large structure is emphasised by the mean streamline that enters the recirculation region close to the ground, and spirals round the vortex tube before leaving close to the top. This also illustrates the fact that mean streamlines can enter the wake (e.g. Hunt, Abell, Peterka & Woo, 1978), and this can be an important factor in determining the average concentration behind the water curtain.

4.3. Vertical profiles

Vertical profiles of the streamwise velocity at several positions along the streamwise axis of symmetry are shown in Fig. 4. The profiles show clearly the region of reverse flow behind the water curtain, which extends to about $L_r/R \sim 2.8$ downwind of the upstream face of the obstacle. A rough estimate for the vertical extent of the recirculating region can be obtained from the heights at which the (positive) velocity gradient is a maximum. This defines a line, almost level with the top of the water curtain, which remains at this height until $x/R \sim 3$, and then falls rapidly to the ground level at $x/R \sim 3.5$. This also coincides with the peak in the production of turbulent energy (Fig. 5), presumably because this is where the mean shear is a maximum. The dissipation is a maximum along this line too (Fig. 6).

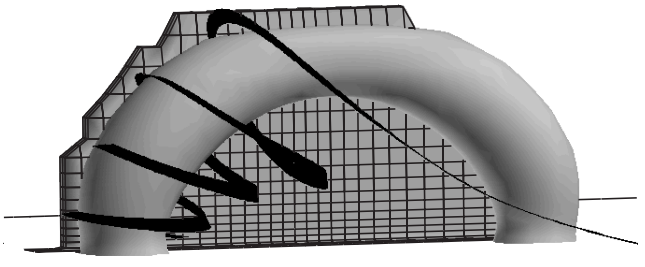

Fig. 3. Visualization of a low pressure iso-surface and streamline behind the curtain, showing the existence of a toroidal vortex structure.

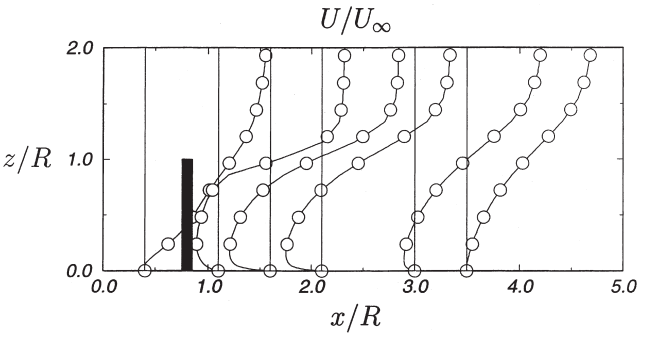

Fig. 4. Profiles of the mean horizontal velocity at several positions downwind of the water curtain.

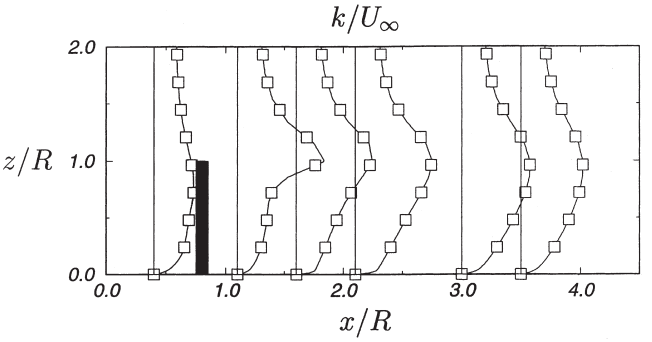

Fig. 5. Profiles of the kinetic energy at several positions downwind of the water curtain.

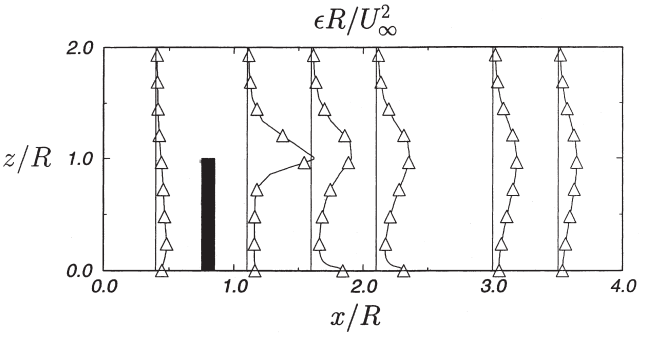

Fig. 6. Profiles of the dissipation at several positions downwind of the water curtain.

5. Concentration field

In order to compare the computed concentrations with those measured in the field experiments of Bara and Dusserre (1997), we have selected four of their tests that were performed in similar conditions. The relevant experimental conditions are given in Table 1. The concentration C will depend on the location of the measurement (x, y, z), the wind speed (say U_r, the velocity at the top of the water curtain), the size of the water curtain (R), the mass flow of ammonia at the source (Q) and a coefficient of turbulent diffusion (K):

$$C = f(x,y,z,U_r,R,Q,K). \tag{1}$$

Now using standard techniques of dimensional analysis, and taking R, U_r and Q as our basic parameters, we obtain:

$$\chi = \frac{CU_rR^2}{Q} = f\left(\frac{x}{R}, \frac{y}{R}, \frac{z}{R}, \frac{K}{U_rR}\right) \tag{2}$$

The coefficient of diffusion, K, can be estimated as u'^2T_L where u' is the rms velocity and T_L is the Lagrangian integral Time Scale, which can in turn be estimated as $\mathscr{L}/u'$ where $\mathscr{L}$ is the integral scale of the turbulence. From which:

$$\frac{K}{U_rR} \sim \frac{u'\mathscr{L}}{U_rR} \tag{3}$$

and it is likely that u'/U_r and $\mathscr{L}/R$ did not vary much over the four field experiments being used for a comparison here, because the size of curtain (R) was kept constant, and for any given type of flow u'/U_r usually remains similar at similar points in the flow. This means that the data from the flow field experiments, expressed in the form

$$\chi = \frac{KCU_rR^2}{Q} = f\left(\frac{x}{R}, \frac{y}{R}, \frac{z}{R}\right) \tag{4}$$

ought to collapse into a single curve.

Transverse profiles of the measured dimensionless concentrations χ are plotted at three positions downwind of the source (x/R = 1.3,2.5,3.5) in Fig. 7(a–c), together with the results from the numerical simulations.

The experimental data do not collapse onto a single curve (Fig. 7(a)) although they exhibit the same tendencies; close to the curtain the concentration drops towards the centreline, but further away, the concentration actually shows a peak on the centreline (Figs. 7(b) and (c)). The biggest differences between the experimental data occur in the profile measured at x/R = 2.5, which is about x/R = 1.7 downstream of the upwind face of the water curtain. There are several possible reasons for the failure of the experimental data to collapse onto a single curve. Firstly, the wind direction and speed fluctuated during the field experiments, and the concentrations were only measured for a period of about 90 s, so the measured concentrations probably do not represent a 'long term' average. This probably also explains why the experimental profiles are rarely symmetrical about the centreline. Secondly, the presence of the water curtain will lead to the formation of large-scale unsteady structures in its wake. A simple calculation for a rigid plate of the same dimensions, in the same flow conditions, suggest that large scale vortices will be shed into the flow at intervals of 25–50 s. This means that the flow downstream of the water curtain is probably influenced rather strongly by large scale unsteady structures with time scales that are rather long compared with the 'averaging time' of the measurements. Once again, then, the measurements probably do not represent a true 'long time' average. (Of course, the question of whether the flow past a rigid plate is a good model for a water curtain in a cross wind remains an important question which we have not been able to investigate here.)

The computed concentration profiles clearly give dimensionless concentrations that are of the same order of magnitude as those measured in the field experiments, which is, in itself, encouraging, because there has been no adjustment of coefficients to force, or improve the agreement. However, it is difficult to go much beyond this 'general agreement'; the numerical model predicts a concentration minimum on the centreline, which might be reproduced in the experimental profiles closest to the water curtain, but is certainly not observed further downwind, where the data show a concentration maximum on the centreline!

Table 1
Experimental conditions for the four cases

Trial	Wind speed (m/s)	Discharge (kg/s)	Comment
1	3.4	4.5	Wind approximately perpendicular to the curtain
2	2.0	7.6	Wind perpendicular to the curtain
3	2.0	7.6	Constant wind speed
4	4.0	7.5	Curtain located 5 m from the release point

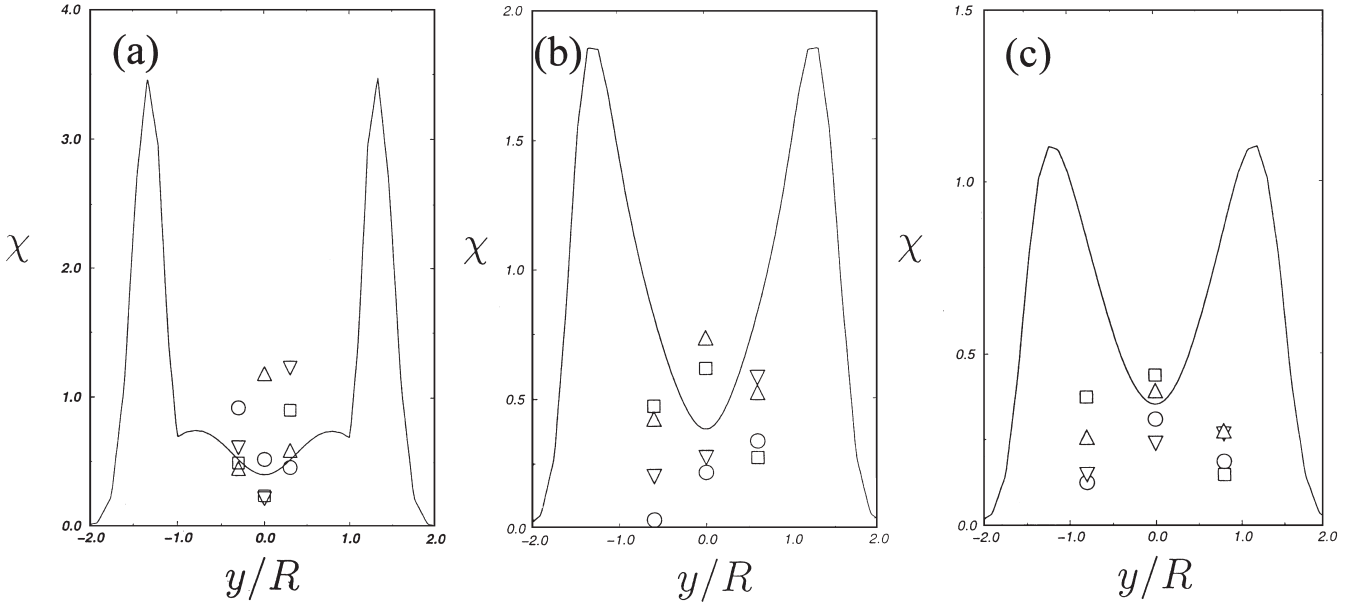

Fig. 7. Transverse profiles of concentration at a height of 0.2 m, at three positions downwind of the release (a) 13 m downwind of the release, (b) 25 m downwind of the release, (c) 35 m downwind of the release. ———, Numerical simulation; ○, Trial 1; □, Trial 2; ▽, Trial 3; △, Trial 4.

The numerical simulations predict very high concentration peaks at the edges of the recirculating region behind the water curtain, but this is not really confirmed by the measurements. Although the measurement positions do not extend outwards sufficiently to provide a definite conclusion, it seems very unlikely that such steep concentration gradients existed in the experiments. There are several possible explanations for this difference. Firstly, the edge of the recirculating region is a zone of very high shear, and the local lateral diffusion of material will be significantly enhanced. This will reduce the peak values and the gradients. Secondly, in the experiments, there was a gap between the ground and the bottom of the water curtain so some ammonia will have been transported into the wake directly, beneath the water curtain (particularly since the ammonia is heavier than air). Also, it is well-known that the phenomenon of 'base bleed' can modify the structure of wake regions significantly.

Another important difference between the experiments and the numerical simulations concerns the unsteadiness of the oncoming flow. Even a nominally 'steady' wind exhibits low frequency fluctuations in direction, so that the effective size of the wake is much larger than that in a truly steady flow. Consequently, the diffusion behind the obstacle is greater than in a steady flow. This may explain why the measured profiles of concentrations in the wake are much flatter than those predicted by the numerical simulations, particularly as the distance downstream of the water curtain increases.

The computed streamwise profile of χ agrees reasonably well with the measured values (Fig. 8). The differences between the computations and the data are generally smaller than the variations between the four experiments, although it is clear that compared with all four experiments, the computations underestimate the concentration immediately downwind of the water curtain.

Another important parameter for defining the performance of the water curtain is the average retention time in the wake. Humphries and Vincent (1976) measured the retention time of smoke in the wake of circular discs, and defined a dimensionless residence time $\tau_r = t_e U_\infty / H$ where t_e is the time for the concentration in the wake to decay by $1/e$, U_∞ is the free stream velocity and H is the characteristic length scale of the object. They found that if the incident flow is smooth $\tau_r \sim 7.4$, and this decreases as the turbulence in the free stream increases. In this simulation, we obtain $\tau_R \sim 6.9$, which is therefore in good agreement with their results. The residence time represents the characteristic time scale for large scale concentration fluctuations in the wake; on the basis of the numerical simulations we estimate that its value in the experiments was of the order of 60 s. Now in the experiments reported by Bara and Dusserre (1997), the measurements began 30 s after release of the ammonia, and lasted for 90 s in total. Thus it seems likely that steady state conditions had not been established in the wake at the start of the measurements, but, on the other hand, the measurement period exceeded the characteristic response time of the wake.

6. Conclusion

The present numerical study shows the capability of a CFD code like Mercure to accurately simulate an

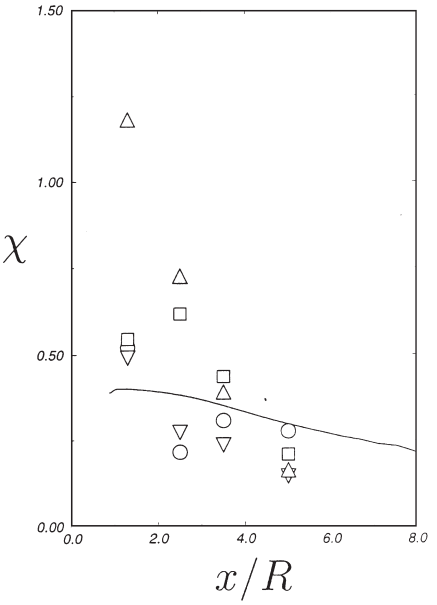

Fig. 8. Longitudinal profile of concentration, at a height of 20 cm. ———, Numerical simulation; ○, Trial 1; □, Trial 2; ▽, Trial 3; △, Trial 4.

ambient ammonia dispersion over a water curtain. The aim of this study was to reproduce the main features of the experiments of Bara and Dusserre (1997). The aerodynamical characteristics of the simulated flow over the curtain are reasonable and we find good agreement between our simulation and other studies from the literature (Corke & Nagib, 1976; Huber & Snyder, 1976). The computed concentration field is also in good agreement with experiments.

These results show that numerical simulations can appreciably complement experiments and provide interesting information to study the efficiency of water curtains.

Acknowledgements

O. Isnard is grateful to the Centre Lyonnais d'Ingénieurie d'Électricité de France for research funding. The authors are also grateful to R.J. Perkins for useful discussions.

References

Bara, A., & Dusserre, G. (1997). *J. Loss Prev. Ind.*, *10*(3), 179–183.

Blewitt, D. N., Yohn, J. F., Koopman, R. P., Brown, T. C., & Hague, W. J. (1987). Effectiveness of water sprays on mitigating anhydrous hydrofluoric-acid releases. In *Internibtion Conference on Vapor Cloud Modeling*, 155–180.

Buty, D., Caneil, J. Y., & Carissimo, B. (1988). *J. Theor. Appl. Mech.*, *2*(7), 35–62.

Corke, T. C., & Nagib, H. M. (1976). Sensitivity of flow around and pressures on a building model to changes in simulated atmospheric surface layer characteristics. IIT Fluid and Heat Transfer–Report R76-1.

Davies, J. K. W. (1992). *J. Hazardous Materials*, *31*,*2*, 177–186.

Hosker R. P. Jr. (1982). Methods for estimating wake flow and effluent dispersion near simple block-like buildings. Oak Ridge, TN: National Oceanic and Atmospheric Administration.

Huber A. H., Snyder W. H. (1976). Building wake effects on short stack effluents. In *Third Symposium an Atmospheric Turbulence, Diffusion and Air Quality*, pp. 235–242 (Boston): American Meteorol. Soc.

Humphries, W., & Vincent, J.H. (1976). *J. Fluid Mech.*, *73*, 453–464.

Hunt J. C. R. (1984). Flow round bluff obstacles. Brussels. Lecture Notes Von Karman Institute.

Hunt, J. C. R., & Mulhearn, P. J. (1973). *J. Fluid Mech.*, *61*, 245–274.

Hunt, J. C. R., Abell, C. J., Peterka, J. A., & Woo, H. (1978). *J. Fluid Mech.*, *86*, 179–200.

Nielsen, M., Ott, S., Jorgensen, H.E., Bengtsson, R., Nyren, K., Winter, S., Ride, D., & Jones, C. (1997). *J. Hazardous Materials*, *56*, 59–105.

Papaspyros, J. N. E., Papanicolaou, P. N., Kastrinakis, E. G. G., & Nychas, S. G. (1996). *J. of Hazardous Materials*, *46*(2,3), 241–252.

Puttock, J. S., & Hunt, J. C. R. (1979). *Atmos. Env.*, *13*, 1–13.

Puttock, J. S. (1979). *Atmos. Env.*, *13*, 15–22.

Woo, H. G. C., Peterka, J. A., & Cermak, J. E. (1977). Wind-tunnel measurements in the wakes structures. NASA Report CR-2806.